Fuel Economy of Hybrid Electric Heavy-Duty Vehicles

Tomaž Katrašnik[*]
University of Ljubljana, Faculty of Mechanical Engineering, Slovenia

Fuel economy of parallel and series hybrid-electric heavy-duty vehicles was analyzed by a combined analytical and simulation approach. The combined approach enables an evaluation of energy flows and energy losses on different energy paths and provides their impact on the fuel economy. The paper quantifies influences of different hybrid-electric vehicle (HEV) topologies, power ratios and characteristics of the components, and applied control strategies on the fuel economy of HEVs. Moreover, the impact of powertrain hybridization on the fuel economy is also analyzed for vehicles carrying different loads operating according to different drive cycles. It is discernable from the results that all of the above parameters significantly influence fuel economy of HEVs. Based on the innovative combined approach the paper reveals and analyzes mechanisms that lead to an optimized fuel economy of hybrid-electric heavy-duty vehicles. Valuable and generally valid guidelines for improving the fuel economy of HEVs are also given.

0 INTRODUCTION

Improvement of the fuel economy is one of the most important issues when developing new vehicle technologies. Among alternative powertrains being investigated, the HEVs consisting of an internal combustion engine (ICE) and an electric machine (EM) are considered to have the best potential in short to mid term future owing to their use of smaller battery pack and their similarities with conventional vehicles [1] and [2]. Hybrid electric heavy-duty vehicles have already proven to have a higher energy conversion efficiency compared to conventional internal combustion engine (ICE) powered vehicles on urban delivery and collection routes, and on bus routes. Although potential fuel economy improvements are much smaller, the introduction of hybrid electric heavy-duty vehicles for extra urban cycles seems promising.

Compared to conventional internal combustion engine vehicles (ICEVs), HEVs incorporate more electrical components featuring many available patterns of combining the power flows to meet load requirements of the vehicle. Dynamic interactions among various components and the multidisciplinary nature lead to complex energy flow patterns among various vehicle components and systems. Modeling and simulation are therefore indispensable for concept evaluation, prototyping, and analysis of HEVs as discussed in [3].

To optimize energy conversion efficiency for particular operating conditions, i.e. drive cycles, it is necessary to have profound knowledge of the influences of the hybrid powertrain topology and of the energy flows through their constituting components on the energy conversion efficiency of the particular HEV. The focus of the paper is, therefore, to analyze influences of the powertrain topology, power ratios and characteristics of the components, drive cycles, control strategies and vehicle loads on the energy conversion efficiency of heavy-duty HEVs applying Li-Ion batteries. The paper reveals and quantifies mechanisms that lead to improved fuel economy of HEVs, and provides guidelines for optimizing fuel economy of HEVs. Energy conversion efficiency of HEVs and ICEVs is analyzed by a combined simulation [4] and analytical [3] approach that enables an analysis of energy flows and energy losses on different energy paths within the powertrain and an evaluation of their influences on the energy consumption of the powertrain.

1 ANALYTICAL FRAMEWORK

Analytical framework was fully derived in [3], therefore only brief resume of equations needed for the presented analysis will be given.

---
[*]Corr. Author's Address: University of Ljubljana, Faculty of Mechanical Engineering, Aškerčeva 6, SI-1000 Ljubljana, Slovenia, tomaz.katrasnik@fs.uni-lj.si
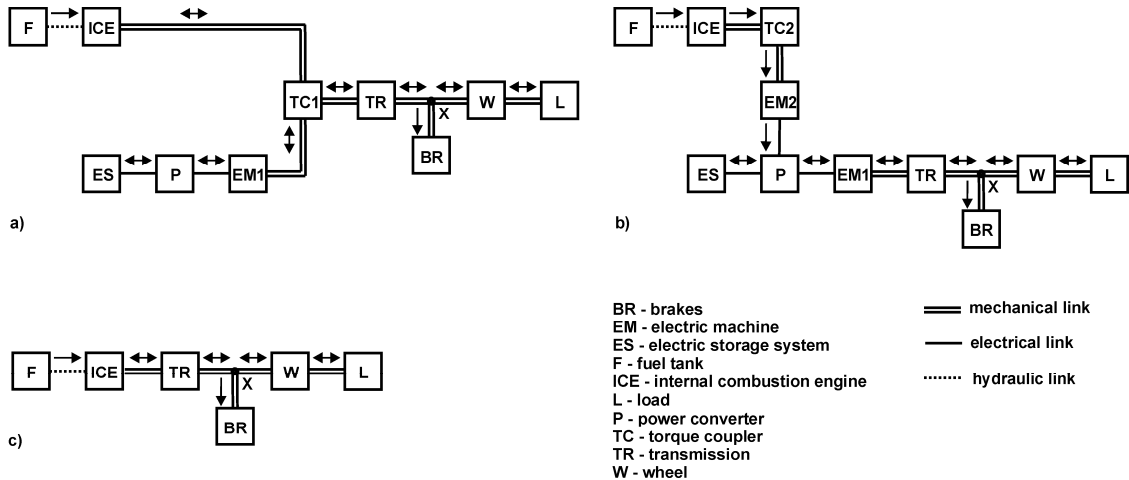
Fig. 1. *Parallel (a), series HEV topology (b) and ICEV topology with indicated energy paths (c)*

The analytical framework considers all energy sources and energy sinks as well as all energy converters including their efficiencies. It thus enables an analysis of energy conversion phenomena considering complex interactions among various components and different control strategies. The advantage of this approach stems from the fact that it considers the complete HEV and therefore enables a direct and insightful evaluation of changes of HEV characteristics and operating conditions on the energy conversion efficiency of the HEV. Input data for the analytical analysis were obtained from the numerical simulations.

It is necessary to divide the HEV, i.e. system, into elements, i.e. subsystems, to investigate energy flows and energy losses and to optimize energy conversion efficiency of the HEV. The elements of the investigated parallel and series HEV topologies, and of the ICEV topology are shown in Fig. 1. A brief introduction of different HEV topologies is given in [3], whereas detailed information could be found in the literature, e.g. [5] and [6]. Energy is added through the fuel tank (F) denoted as "energy sources". Energy is extracted through the load (L) and the brakes (BR), denoted as "energy sinks". All other elements are denoted as "energy converters". There exist unidirectional and bidirectional energy paths in the hybrid electric vehicle as indicated by the arrows in Fig. 1. It is assumed that energy can not be accumulated in the links.

Analysis of the fuel consumption is commonly performed for a specific test cycle. Therefore, all energy flows between the elements are integral values over the whole test cycle (tc). It is assumed that all losses that occur in the links between elements are included in the losses of the elements. The energy flow between arbitrary elements A and B is denoted W_{A-B} and considers only the energy flow from A to B, whereas the energy flow from B to A is considered by W_{B-A}. Efficiencies of the elements without energy accumulation capability with two bidirectional energy links are defined as the ratio between downstream and upstream energy flow. The efficiency index of such elements firstly indicates the element, and secondly, the direction of the energy flow, i.e. *PR* - propulsion and *BR* - braking. It is more complex to define efficiencies of the elements with more than two bidirectional energy links, i.e. TC and P, and elements with energy accumulation capability, i.e. ES; Fig. 1. Energy losses of these elements are split into inlet and outlet losses to make a clear derivation of equations possible. In order to perform this analysis, a point inside the element that represents the origin for evaluating the energy balance is defined; more details are given in [3]. The efficiency index of such elements thus indicates firstly, the element, secondly, losses associated with inflow or outflow of the energy, i.e. *in* or *out*, and thirdly, the energy path. Energy flow to the element with more than two links could be split into energy flow to two or more subsequent elements; for example energy flow ICE-TC1 in

parallel HEV (Fig. 1) could be split into energy flow ICE-TC1-TR (vehicle propulsion) and to energy flow ICE-TC1-EM1 (charging the EM by the ICE). These energy flows are denoted $W'_{ICE-TC1,TR}$ for the energy path ICE-TC1-TR and $W'_{ICE-TC1,TR}$ for the energy path ICE-TC1-EM1. It follows that $W'_{ICE-TC1,TR} = W_{ICE-TC2} - W'_{ICE-TC1,EM1}$, where »'« indicates that this is only a portion of the energy flow denoted by the first index directed to the element referred to by the second index.

Energy content of the electric storage devices at the end of the test cycle was equal to the energy content of the electric storage devices at the beginning of the test cycle (denoted non-depleting ES management), and plug-in option was not considered to enable a clear and demonstrative comparison of the fuel economy. A multiplication factor, i.e. F, defined as a ratio of the propulsion work over the test cycle for arbitrary vehicle topology to the propulsion work over the test cycle for ICEV is introduced. Therefore $F=1$ for ICEVs, whereas generally $F \neq 1$ for HEVs due to difference in vehicle parameters (vehicle mass, drag coefficient). Introduction of

multiplication factors enables comparison of the energy consumptions of different vehicle topologies, since it makes possible scaling of the propulsion work over the test cycle ($W_{tc,PR}$) of different HEV topologies to $W_{tc,PR}$ of the ICEV, i.e. $[W_{tc,PR}]_P = F_P[W_{tc,PR}]_I$ and $[W_{tc,PR}]_S = F_S[W_{tc,PR}]_I$. Index I denotes internal combustion engine vehicle, index S denotes the parallel HEV and index S denotes series HEV.

ICEVs are the most widespread type of vehicles and therefore they often represent the basis for the evaluation of the energy consumption of other vehicle topologies. The ratio of the fuel consumptions of parallel HEV and ICEV topology was derived in [3] where $m_{f,tc}$ is the mass of fuel consumed over the test cycle, η efficiency, Q_{LHV} lower heating value of the fuel, indexes G and M denote operation of the EM in the generator and in the motor mode respectively, and other indexes denote elements in Fig. 1 according to the rules addressed above.

Similarly, fuel consumption ratio for series HEV and ICEV topology reads [3] in Eq. (2).

$$
\frac{[m_{f,tc}]_P}{[m_{f,tc}]_I} = \left\{ \frac{[\eta_{ICE,eff}\eta_{TR,PR}\eta_{W,PR}]_I}{[\eta_{ICE,eff}\eta_{TC1,in,ICE-TC1}\eta_{TC1,out,TC1-TR}\eta_{TR,PR}\eta_{W,PR}]_P} \right\}_{REFW}
$$

$$
\times \left\langle \{F_P\}_{TcPrR} + \left\{ \frac{1}{[m_{f,tc}Q_{LHV}\eta_{ICE,eff}\eta_{TR,PR}\eta_{W,PR}]_I} \left(F_P [W_{TR-ICE}\eta_{TR,PR}\eta_{W,PR}]_I \right. \right. \right.
$$

$$
\left. \left. - [W'_{TR-TC1,ICE}\eta_{TC1,in,TR-TC1}\eta_{TC1,out,TC1-ICE}\eta_{TC1,in,ICE-TC1}\eta_{TC1,out,TC1-TR}\eta_{TR,PR}\eta_{W,PR}]_P \right) \right\}_{MIce} \tag{1}
$$

$$
- \left\{ \frac{[W_{tc,BR} - W_{BR}/\eta_{W,BR} - W'_{TR-TC1,ICE}/(\eta_{W,BR}\eta_{TR,BR})]_P}{[m_{f,tc}Q_{LHV}\eta_{ICE,eff}\eta_{TR,PR}\eta_{W,PR}]_I} [\eta_{W,BR}\eta_{TR,BR}\eta_{TC1,in,TR-TC1}\eta_{TC1,out,TC1-EM1}\eta_{EM1,G}\eta_{P,in,EM1-P} \right.
$$

$$
\times \eta_{P,out,P-ES}\eta_{ES,in,P-ES}\eta_{ES,out,ES-P}\eta_{P,in,ES-P}\eta_{P,out,P-EM1}\eta_{EM1,M}\eta_{TC1,in,EM1-TC1}\eta_{TC1,out,TC1-TR}\eta_{TR,PR}\eta_{W,PR}]_P \Big\}_{RB}
$$

$$
+ \left\{ \frac{[W'_{ICE-TC1,EM1}]_P}{[m_{f,tc}Q_{LHV}\eta_{ICE,eff}\eta_{TR,PR}\eta_{W,PR}]_I} [\eta_{TC1,in,ICE-TC1}(1 - \eta_{TC1,out,TC1-EM1}\eta_{EM1,G}\eta_{P,in,EM1-P}\eta_{P,out,P-ES} \right.
$$

$$
\times \eta_{ES,in,P-ES}\eta_{ES,out,ES-P}\eta_{P,in,ES-P}\eta_{P,out,P-EM1}\eta_{EM1,M}\eta_{TC1,in,EM1-TC1})\eta_{TC1,out,TC1-TR}\eta_{TR,PR}\eta_{W,PR}]_P \Big\}_{CEsIce} \right\rangle .
$$

$$
\frac{\left[m_{f,tc}\right]_S}{\left[m_{f,tc}\right]_I} = \left\{ \frac{\left[\eta_{ICE,eff}\eta_{TR,PR}\eta_{W,PR}\right]_I}{\left[\eta_{ICE,eff}\eta_{TC2,in,ICE-TC2}\eta_{TC2,out,TC2-EM2}\eta_{EM2,G}\eta_{P,in,EM2-P}\eta_{P,out,P-EM1}\eta_{EM1,M}\eta_{TR,PR}\eta_{W,PR}\right]_S} \right\}_{REFW}
$$

$$
\times \left\langle \{F_S\}_{TcPrR} + \left\{ \frac{F_S\left[W_{TR-ICE}\eta_{TR,PR}\eta_{W,PR}\right]_I}{\left[m_{f,tc}Q_{LHV}\eta_{ICE,eff}\eta_{TR,PR}\eta_{W,PR}\right]_I} \right\}_{MIce} \right.
$$

$$
- \left\{ \frac{\left[\left(W_{tc,BR}-W_{BR}/\eta_{W,BR}\right)\right]_S}{\left[m_{f,tc}Q_{LHV}\eta_{ICE,eff}\eta_{TR,PR}\eta_{W,PR}\right]_I} \left[\eta_{W,BR}\eta_{TR,BR}\eta_{EM1,G}\eta_{P,in,EM1-P}\eta_{P,out,P-ES}\eta_{ES,in,P-ES}\eta_{ES,out,ES-P}\right.\right. \tag{2}
$$

$$
\left.\left.\times\eta_{P,in,ES-P}\eta_{P,out,P-EM1}\eta_{EM1,M}\eta_{TR,PR}\eta_{W,PR}\right]_S\right\}_{RB}
$$

$$
+ \left\{ \frac{\left[W'_{EM2-P,ES}\right]_S}{\left[m_{f,tc}Q_{LHV}\eta_{ICE,eff}\eta_{TR,PR}\eta_{W,PR}\right]_I}\left[\eta_{P,in,EM2-P}\left(1-\eta_{P,out,P-ES}\eta_{ES,in,P-ES}\eta_{ES,out,ES-P}\eta_{P,in,ES-P}\right)\right.\right.
$$

$$
\left.\left.\times\eta_{P,out,P-EM1}\eta_{EM1,M}\eta_{TR,PR}\eta_{W,PR}\right]_S\right\}_{CEsIce} \right\rangle .
$$

It can be concluded from Eqs. (1) and (2) that both HEVs utilize fuel energy more efficiently than ICEV if

$$
\frac{\left[m_{f,tc}\right]_{HEV}}{\left[m_{f,tc}\right]_I} < 1, \tag{3}
$$

whereas right-hand-side (rhs) of both equations reveals and quantifies the mechanisms that could lead to this goal; index *HEV* represents *P* or *S*. In Eqs. (1) and (2), *REFW* (**R**atio of **E**fficiencies of the energy conversion chains from **F**uel tank to **W**heels) term represents the ratio of efficiencies of the energy conversion chains from the fuel tank (F) to wheels (W) of the ICEV topology and the particular HEV topology. The nominator and the denominator of *REFW* term thus include efficiencies of all converter elements in the energy conversion chain from F to W for the particular vehicle topology (Fig. 1). *REFW* term is multiplied by the sum of the terms: *TcPrR* (**T**est **c**ycle **Pr**opulsion work **R**atio), *MIce* (**M**otoring **I**nternal **c**ombustion **e**ngine), *RB* (**R**egenerative **B**raking) and *CEsIce* (**C**harging **E**lectric **s**torage devices by the **I**nternal **c**ombustion **e**ngine). *TcPrR* term is equal to the multiplication factor of the test cycle, F_P or F_S, that is generally larger than unity due to a larger vehicle mass of the HEVs as discussed above. This term thus, tends to decrease the energy conversion efficiency of both HEV topologies. *MIce* term considers the difference of energies delivered to the ICE of observed vehicle topologies by the external torque. Motoring of the

ICE by external torque rather than by fuel addition clearly reduces the fuel consumption of the ICEV. Series HEV topology does not enable motoring of the ICE by the external torque originating from the vehicle inertia, since ICE is not mechanically coupled to the wheels as it is discernable from Fig. 1. *MIce* thus clearly increases the ratio $[m_{f,tc}]_S/[m_{f,tc}]_I$ in Eq. (2). In parallel HEV, *MIce* term generally increases the ratio $[m_{f,tc}]_S/[m_{f,tc}]_I$, Eq. (1), since parallel HEVs incorporate downsized ICEs featuring smaller energy consumption capability. It should be noted that energy consumed by the ICE in the ICEV could be used for regenerative braking in both HEV topologies. Additionally, control strategies of the parallel HEV attempt to avoid the operation of the ICE at low loads and correspondingly at low efficiency of the ICE, thereby reducing the amount of the energy consumed by the ICE through motoring by external torque. For HEVs, negative effects due to the *MIce* term are therefore generally overcompensated by positive effects due to regenerative braking (*RB*), higher $\eta_{ICE,eff}$, and lower losses due to charging ES by the ICE (*CEsIce*). *RB* term considers regenerative braking, which is one of the major mechanisms for increasing energy conversion efficiency of both HEV topologies. It is obvious that increase in the energy conversion efficiency is proportional to the amount of the energy available for regenerative braking. $\left[W_{tc,BR}-W_{BR}/\eta_{W,BR}\right]_S$ of the series HEV is generally larger than

$\left[W_{tc,BR} - W_{BR}/\eta_{W,BR} - W'_{TR-TC1,ICE}/\left(\eta_{W,BR}\eta_{TR,BR}\right)\right]_P$ of the parallel HEV, since EM1 in the series HEV needs to be sized for a maximum power output of the HEV and thus enables recuperation of larger amount of the energy through regenerative braking. *CEsIce* accounts for the losses due to charging the ES by the energy produced by the ICE. It therefore obviously decreases energy conversion efficiency of both HEV topologies.

Additionally, analytical framework for comparing conventional ICEV and ICEV featuring stop/start strategy (denoted I,SS) is given in [3]:

$$\frac{\left[m_{f,tc}\right]_{I,SS}}{\left[m_{f,tc}\right]_I} = \left\{\frac{\left[\eta_{ICE,eff}\eta_{TR,PR}\eta_{W,PR}\right]_I}{\left[\eta_{ICE,eff}\eta_{TR,PR}\eta_{W,PR}\right]_{I,SS}}\right\}_{REFW}$$

$$\times\left\langle\left\{F_{I,SS}\right\}_{TcPrR} + \left\{\frac{1}{\left[m_{f,tc}Q_{LHV}\eta_{ICE,eff}\eta_{TR,PR}\eta_{W,PR}\right]_I}\right\}\right. \quad (4)$$

$$\times\left(F_{I,SS}\left[W_{TR-ICE}\eta_{TR,PR}\eta_{W,PR}\right]_I\right.$$

$$\left.\left.-\left[W_{TR-ICE}\eta_{TR,PR}\eta_{W,PR}\right]_{I,SS}\right)\right\}_{MIce}\right\rangle.$$

Generally mass of the vehicle does not change significantly with the introduction of the stop/start strategy, therefore, *TcPrR*→1. If an additionally equal driver model is applied, then *MIce*→0. Therefore, introduction of the stop/start strategy influences *REFW* term through $\eta_{ICE,eff}$ and increases energy conversion efficiency of ICEV featuring stop/start strategy. *RB* and *CEsIce* terms are not considered in Eq. (4), since these mechanisms are not inherent to either of the vehicle topologies compared in Eq. (4).

2 SIMULATION MODEL

A forward-facing model was applied for modeling of ICEV and both HEV topologies. Simulation models for ICE powertrain and both hybrid powertrains were described in detail in [7] and [8], whereas an extended simulation model incorporating sub-models of additional components required for modeling vehicle dynamics and corresponding control strategies

was proposed in [4]. Therefore, the models are only briefly summarized subsequently.

Analyses were performed for a MAN 8.225 LC truck equipped with a six gear S6-850 gearbox representing a baseline ICEV. Vehicle mass amounts to 3485 kg, whereas maximum gross mass equals 7490 kg. Simulations were performed for a fully loaded vehicle, for a vehicle carrying no load and for vehicle carrying half of the maximum payload to expose influences of the vehicle mass on the energy conversion efficiency. When modeling HEVs, mass increase due to additional batteries, electric machines and other electric accessories is considered, as well as mass decrease due to downsizing ICE in both HEV topologies, and omission of the gear box in the series HEV. Masses of HEVs are thus larger than masses of the ICEV, however this approach enables a comparison of the energy consumption for equal payloads.

The MAN D0826 LOH 15 turbocharged diesel engine (max. torque 862 Nm at 1400 rpm, max. power 158 kW at 2400 rpm) is applied as the baseline internal combustion engine. The ICEs with $R_V = V_{downsized} / V_{baseline}$ equal to 0.8 and 0.5 were analyzed with the parallel HEV, and the ICE with $R_V = 0.5$ was analyzed with the series HEV; V is swept volume of the ICE.

The ENAX Li-Ion High Power 3.8 V, 2 Ah cell is applied as the module of the Li-Ion storage system. A prototype electric motor-generator presented in [7] was applied in the parallel hybrid powertrain and as an electric motor in the series one. Characteristics of the STAMFORD UCM 274F (max. input power 94.6 kW, max. efficiency 93%) were used to simulate an electric generator in the series hybrid powertrain.

Components of the analyzed HEVs were sized according to the following constraint $\left(M_{ICE,h} + M_{EM}\right)_{n\left(M_{ICE,b,\max}\right)} = M_{ICE,b}\big|_{n\left(M_{ICE,b,\max}\right)}$ for the parallel HEV, and

$M_{EM}\big|_{n\left(M_{ICE,b,\max}\right)} = M_{ICE,b}\big|_{n\left(M_{ICE,b,\max}\right)}$ for the series one, M is torque and $n\left(M_{ICE,b,\max}\right)$ represents engine speed that corresponds to the maximum torque of the baseline ICE engine.
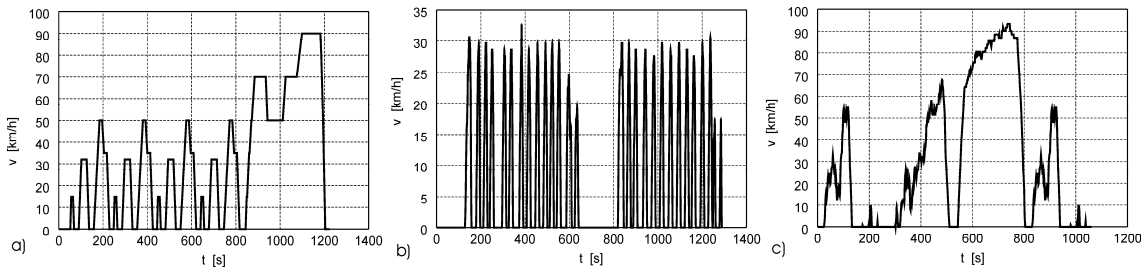
Fig. 2. *Velocity profile of: a) ECE_EUDC_LOW, b) BUSRTE, and c) UDDSHDV cycles*

Energy losses and thus efficiency of the tire are evaluated by the rolling resistance momentum model of the tire that was modeled according to model proposed in [9]. In the proposed analysis both HEV topologies do not incorporate torque couplers (TC). In the series HEV, ICE is directly mechanically connected to the EM2, whereas in parallel HEV, EM1 operates in the same speed range as ICE and it could therefore be directly mechanically coupled to the shaft.

Two control strategies were applied to ICEVs: 1) normal operation of the ICEV, and 2) ICEV with stop/start control strategy (denoted SS).

All parallel HEVs apply SS control strategy. Additionally, two different regimes of vehicle propulsion during drive-away and at low powertrain loads were analyzed: 1) ICE solely provides the torque for vehicle propulsion up to maximum torque output of the ICE, and 2) EM solely provides the torque up to a specified limit and afterwards ICE solely provides the torque for vehicle propulsion up to the maximum torque output of the ICE. The latter control strategy is denoted as EM_START. This control strategy avoids operation of the ICE in the inefficient regions [4] and [10]. The control strategy of the parallel HEV allows for: 1) drive-away and vehicle propulsion by EM at low powertrain loads if EM_START operating regime is enabled, 2) ICE and EM deliver power in parallel if ICE is not able to provide a required power output, 3) replenishing the batteries by operating the ICE at a higher torque output, 4) regenerative braking, 5) simultaneous operation of the ICE and the EM in order to prevent charging of the batteries above the specified limit, and 6) normal operation of the ICE.

The ICEs of the series HEVs were operated according to the optimum engine operation line (OEOL) [6]. In the presented analysis the power output of the ICE operating according to OEOL was based on the battery state-of-charge (SOC), i.e. fuel rack (FR)∝SOC, and engine speed (n)∝FR as presented in Ref. [4]. Corresponding to the OEOL two control strategies were applied to series HEVs [4]: 1) ICE is turned on and off according to the SOC (denoted CS_S_SOC), and 2) ICE is turned on and off according to the characteristics of the test cycle, i.e. ICE is turned on during the vehicle propulsion period and it is turned off during vehicle stops and during regenerative braking (denoted CS_S_tc). These two control strategies were introduced to analyze influences of the energy flow $W'_{EM2-P,ES}$ Eq. (2), i.e. charging the ES by the ICE, on the energy conversion efficiency of the series HEV. CS_S_tc ensures a smaller energy flow through the ES, however it also decreases maximum sustained power.

3 TEST CYCLES

Three different test cycles were analyzed to investigate the influences of the test cycle characteristics on energy conversion efficiency of different HEV topologies and configurations [11]: ECE+EUDC (NEDC) for low-powered vehicles (ECE_EUDC_LOW), Fig. 2a), 2.65 km bus route with 28 stops (BUSRTE), Fig. 2b, and Urban Dynamometer Driving Schedule for Heavy-Duty Vehicles (UDDSHDV) Fig. 2c. By comparing ECE_EUDC_LOW and BUSRTE cycle it can be observed that the latter features a significantly lower average velocity, frequent decelerations to stand-still and longer vehicle stop period. The average velocity of the ECE_EUDC_LOW is similar to that of the UDDSHDV, however UDDSHDV cycle features more frequent and more severe accelerations.

4 RESULTS

The results for three vehicle topologies giving eight different configurations carrying different loads and driven according to three different test cycles are shown in this section. Only the results of powertrain configurations that are able to comply with non-depleting ES management strategy are shown in order to enable credible comparison of energy conversion efficiencies.

The relative change in the fuel consumption, $\Delta m_{f,X}$ could also be written as the sum of the products of the *REFW* term with terms *TcPrR*, *MIce*, *RB* and *CEsIce*, where a particular term reveals the influence of a particular mechanism on the $\Delta m_{f,X}$. It follows:

$$\Delta m_{f,X} = \frac{\left[m_{f,tc}\right]_X}{\left[m_{f,tc}\right]_I} - 1$$

$$= \left[\underbrace{\left(REFW \times TcPrR - 1\right)}_{TcPrR*} + \underbrace{REFW \times MIce}_{MIce*} \right. \quad (5)$$

$$\left. + \underbrace{REFW \times RB}_{RB*} + \underbrace{REFW \times CEsIce}_{CEsIce*} \right],$$

where *X* represents *P* or *S* or *I,SS*. Terms larger than 0 indicate an increase in the $\Delta m_{f,X}$, and terms smaller that 0 indicate a decrease in the $\Delta m_{f,X}$. Additionally, the vehicle mass ratio

$$\Delta m_{V,X} = \frac{m_{V,X}}{m_{V,I}} - 1 \quad (6)$$

is introduced to reflect change in the vehicle mass relative to the mass of the ICEV. In the subsequent text indexes are not written with the parameters introduced in Eqs. (5) and (6), since it is discernable from the accompanying text and figures which topology and configuration is analyzed.

The following notation is adopted in this section: ICEV – internal combustion engine vehicle, ICEV_SS – internal combustion engine vehicle with stop/start (SS) strategy, PHEV_Rv = 0.8_EM = 0 – parallel HEV incorporating ICE with $R_V = 0.8$ without EM_START strategy, PHEV_Rv = 0.8_EM = 1 – parallel HEV incorporating ICE with $R_V = 0.8$ with EM_START strategy, PHEV_Rv = 0.5_EM = 0 – parallel HEV incorporating ICE with $R_V = 0.5$ without

EM_START strategy, PHEV_Rv = 0.5_EM = 1 – parallel HEV incorporating ICE with Rv = 0.5 with EM_START strategy, SHEV_SOC – series HEV with CS_S_SOC strategy, and SHEV_tc – series HEV with CS_S_tc strategy.

4.1 ECE_NEDC_LOW Cycle

Figs. 3a to 3c shows parameters of fully loaded vehicles driven according to the ECE_NEDC_LOW cycle: a) relative change in fuel consumption (Δm_f), effective efficiency of the ICE ($\eta_{ICE,eff}$), and Δm_V introduced in Eq. (6), b) *TcPrR**, *MIce**, *RB** and *CEsIce**, parameters introduced in Eq. (5), and c) energy needed for vehicle propulsion ($W_{tc,PR}$), energy needed for braking the vehicle (integral over negative values of the test cycle power trace - $W_{tc,PR}$) and energy consumed by the brakes (W_{BR}), whereas in Figs. 3d to 3f the same parameters are shown for an empty vehicle. PHEV_Rv = 0.5_EM = 1 was not able to comply with non-depleting ES management when fully loaded, since ICE could not provide enough energy to replenish the ES in the period when it was turned on. These results are therefore not shown in Figs. 3a to c.

It is discernable from the results that different topologies and configurations significantly influence fuel economy of HEVs (Δm_f – Figs. 3a and d). It can also be observed that HEVs featuring the highest $\eta_{ICE,eff}$ and recuperating the largest amount of energy by regenerative braking (indicated by *RB** and by the difference between $W_{tc,BR}$ and W_{BR}) do not necessarily feature the highest fuel economy. It is therefore necessary to analyze particular terms of Eq. (5) to explain the influence of the energy conversion phenomena along different energy paths on the fuel consumptions of particular vehicle topology.

It is discernable from Figs. 3c and f that vehicle mass of parallel HEVs increases with an increasing hybridization factor and that series HEVs feature larger vehicle mass due to an application of two electric machines and due to a larger number of battery modules. Δm_v values differ for fully loaded and empty HEVs, since additional mass due to powertrain hybridization is constant and $\Delta m_{V,I}$ Eq. (6) changes with the vehicle load. $W_{tc,PR}$ and $W_{tc,BR}$ (Figs. 3c and f) increase corresponding to the vehicle mass.
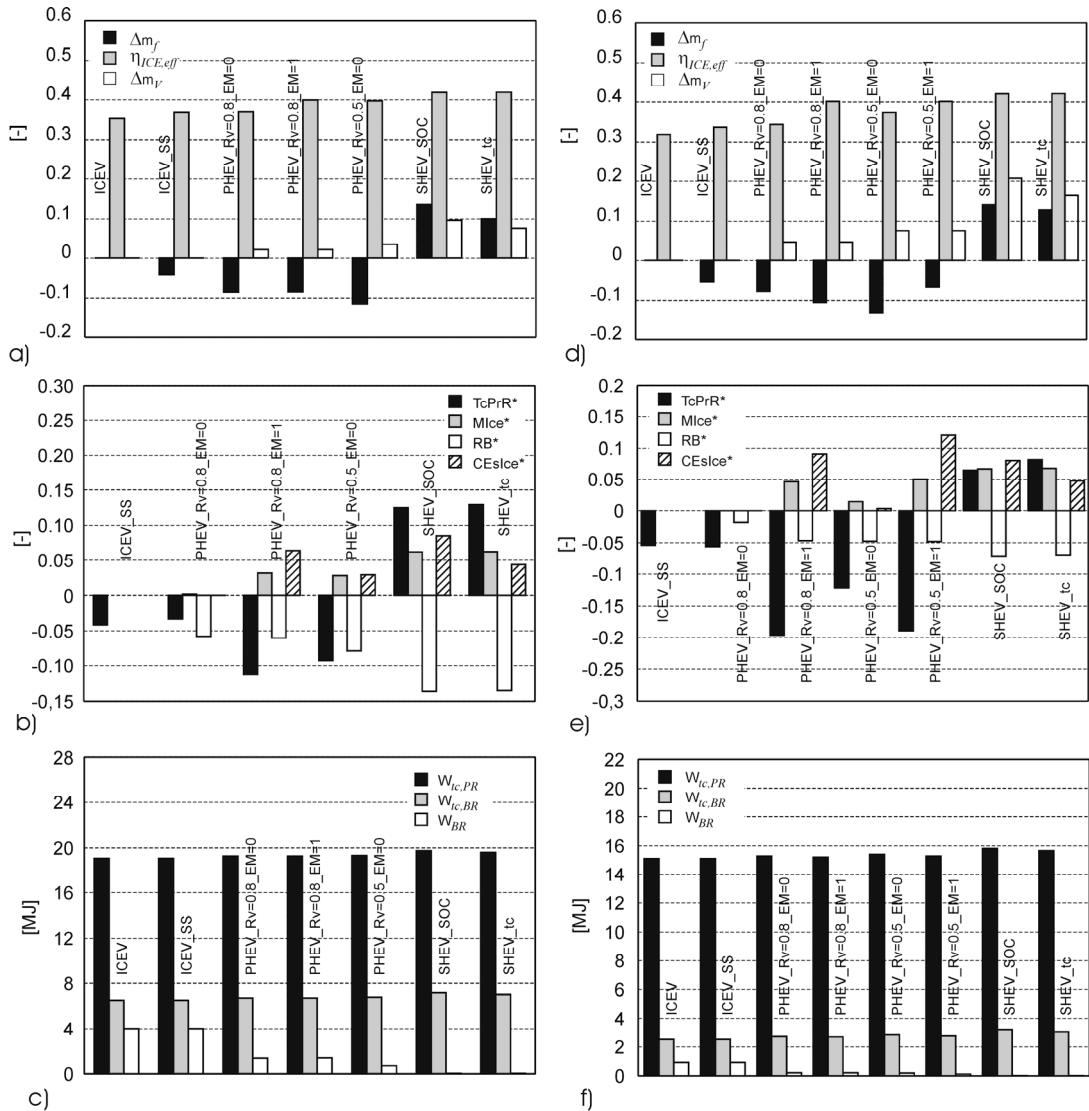
Fig. 3. *ECE_NEDC_LOW cycle: a) Δm$_f$, η$_{ICE,eff}$ and Δm$_V$ b) TcPrR*, Mice*, RB* and CEsIce* and c) W$_{tc,PR}$, W$_{tc,BR}$ and W$_{BR}$ for fully loaded vehicle, and d) to f) the same parameters for an empty vehicle*

It can be observed from Figs. 3a and d that fuel economy improvement of ICEV_SS and all HEVs over ICEV is slightly larger for the empty vehicle compared to the fully loaded vehicle

However, by analyzing particular terms of Eq. (5) it can be concluded that the contribution of different mechanisms to the relative change in the fuel consumption (Δm$_f$) is significantly influenced by the vehicle load. It is discernable that lower vehicle mass results in lower values of W$_{tc,PR}$ and W$_{tc,BR}$, which is quite obvious (Figs. 3c

and f). However, the ratio between W$_{tc,BR}$ and W$_{tc,PR}$ also decreases for the empty vehicle, since relatively more energy is consumed to overcome the aerodynamic drag. The ratio between W$_{tc,BR}$ and W$_{tc,PR}$ significantly influences relative amount of the energy available for regenerative braking and thus the term RB*. Therefore, regenerative braking posses a smaller potential to improve the fuel economy of lighter vehicles. It is discernable from Figs. 3a and d that η$_{ICE,eff}$ of the ICEV is lower for the empty vehicle compared to the fully

Katrašnik, T.

loaded one, which is also quite obvious since lower torque is needed to drive an empty vehicle according to a specified velocity trace resulting in lower $\eta_{ICE,eff}$. Therefore, a relative improvement in $\eta_{ICE,eff}$ of ICEV_SS and all HEVs over ICEV is more pronounced for the empty vehicle. This phenomenon mainly influences lower values of *TcPrR** for the empty vehicle.

It is discernable from Figs. 3a and d that stop/start strategy increases $\eta_{ICE,eff}$ and therefore improves the fuel economy of the fully loaded and empty ICEV_SS, since other vehicle parameters are equal for ICEV_SS and ICEV.

Fig. 3 shows that fully loaded and empty PHEV_Rv = 0.8_EM = 0 and PHEV_Rv = 0.8_EM = 1 feature improved fuel economy (Δm_f) over ICEV and over ICEV_SS. It can also be seen that the difference in Δm_f of PHEV_Rv = 0.8_EM = 1 and PHEV_Rv = 0.8_EM = 0 is much smaller than difference in $\eta_{ICE,eff}$. The operation according to the EM_START (PHEV_Rv = 0.8_EM = 1) strategy avoids inefficient engine operating conditions and thus results in higher $\eta_{ICE,eff}$. However, the operation according to the EM_START strategy also implies higher electric energy consumption by the EM, and thus ES are also charged by the ICE (*CEsIce**>0), since regenerative braking alone does not provide enough electric energy to operate the HEV according to the non-depleting ES management strategy. Moreover, these facts result also in *MIce**>0, since ICE is less frequently motored by external torque due to an operation at a higher torque output to replenish the batteries. PHEV_Rv = 0.8_EM = 0 thus features an improved fuel economy over ICEV_SS mainly due to regenerative braking (*RB**<0). PHEV_Rv = 0.8_EM = 1 features improved fuel economy over ICEV_SS due to higher $\eta_{ICE,eff}$, whereas all other mechanisms, i.e. *TcPrR+MIce+RB+CEsIce*>1 in Eq. (1), deteriorate its fuel economy.

It is discernable from Fig. 3 that a fully loaded and empty PHEV_Rv = 0.5_EM = 0 features the highest fuel economy for the ECE_NEDC_LOW cycle. PHEV_Rv = 0.5_EM = 0 consumes less fuel than PHEV_Rv = 0.8_EM = 0 due to higher $\eta_{ICE,eff}$ and due to a larger amount of the energy recuperated by regenerative braking. The first improvement arises from the application of the downsized ICE featuring higher $\eta_{ICE,eff}$, whereas the latter improvement arises from the application of a more powerful EM that is capable of recuperating more energy by regenerative braking. PHEV_Rv = 0.5_EM = 0 consumes less fuel than PHEV_Rv = 0.8_EM = 1 mainly due to lower losses associated with charging the ES by the ICE (*CEsIce**) and due to a larger amount of the energy recuperated by regenerative braking (*RB**). It can be observed that empty PHEV_Rv = 0.5_EM = 1 vehicle consumes more fuel than empty PHEV_Rv = 0.5_EM = 0 vehicle, since improvement in $\eta_{ICE,eff}$ is smaller than losses associated with charging the ES by the ICE.

EM_START strategy thus improves fuel economy of the parallel HEV with $R_V = 0.8$ and deteriorates fuel economy of the parallel HEV with $R_V = 0.5$. It can generally be concluded that EM_START strategy leads to improved fuel economy if improvement in $\eta_{ICE,eff}$ overcompensates negative influences of charging the ES by the ICE (*CEsIce**) and smaller energy consumption of the energy by motoring the ICE by external torque (*MIce**).

It is instructive to compare values of the *CEsIce** terms for PHEV_Rv = 0.8_EM = 1 and PHEV_Rv = 0.5_EM = 0 for both vehicle loads. *CEsIce** of the empty PHEV_Rv = 0.8_EM = 1 vehicle is larger than *CEsIce** of a fully loaded PHEV_Rv = 0.8_EM = 1 vehicle, since *RB** term is smaller indicating that relatively less energy is recuperated by regenerative braking and thus, more energy from ICE is needed to charge the ES thereby enabling an operation according to the EM_START strategy. Opposite, *CEsIce** for the empty PHEV_Rv = 0.5_EM = 0 vehicle is smaller than *CEsIce** for the fully loaded PHEV_Rv = 0.5_EM = 0 vehicle, since lower torque is needed to drive an empty vehicle according to a specified velocity trace and thus EM power assist is smaller.

Fuel consumption of all series HEVs exceed that of the ICEV despite the highest value of $\eta_{ICE,eff}$ and the largest amount of the energy recuperated by regenerative braking (difference between $W_{tc,BR}$ and W_{BR}). This is the consequence of a lower efficiency of the energy conversion chain from F to W and to a lesser extent, a consequence of larger vehicle mass. Both effects result in *TcPrR**>0. Increase in $\eta_{ICE,eff}$ of the series HEVs is thus not high enough to overcompensate drawbacks of the longer energy

conversion chain incorporating EM2, P and EM1 (REFW term in Eq. (2)). Despite the largest amount of the energy recuperated by regenerative braking, $TcPrR+MIce+RB+CEsIce>1$ (eq. (2)) due to larger vehicle mass (Δm_V) that results in a higher $W_{tc,PR}$ value, due to losses associated with charging the ES by the ICE (CEsIce*), and due to MIce*>0 (since series HEVs do not incorporate the mechanism of energy consumption by the ICE). Larger vehicle mass of the series HEVs is mainly related to a larger number of battery stacks being required due to higher charging currents.

4.2 Influence of the Vehicle Load and of the Drive Cycle Characteristics on the Fuel Economy

Fig. 4 shows Δm_f for different relative loads (0 – empty vehicle, 1 – fully loaded vehicle) operating according to the a) ECE_NEDC_LOW, b) BUSRTE and c) UDDSHDV cycle. It is discernable from the results that drive cycle influences fuel economy improvement of HEVs more significantly than vehicle load.

From Fig. 4a it can be concluded that Δm_f of the ICEV_SS decreases with increasing vehicle load, since a relative amount of the fuel consumed during idling also decreases with an increased vehicle load. It can be seen that Δm_f curve of the PHEV_Rv = 0.8_EM = 0 features a negative slope, since positive effect due to a relatively larger amount of the energy available for regenerative braking at high vehicle loads overcompensate negative effects due to smaller improvement in $\eta_{ICE,eff}$ as discernable in Fig. 3. On the other hand, Δm_f curves of the PHEV_Rv = 0.8_EM = 1 and PHEV_Rv = 0.5_EM = 0 feature a positive slope, since positive effects due to a relatively larger amount of the energy available for regenerative braking at high vehicle loads are smaller than negative influences due to a smaller improvement in $\eta_{ICE,eff}$ and due to charging the ES by the ICE (Fig. 3). Δm_f curves of series HEVs are mainly characterized by the trade-off between an improvement in $\eta_{ICE,eff}$ and thus, an improvement in the energy conversion efficiency from F to W, and regenerative braking (RB*- Fig. 3).
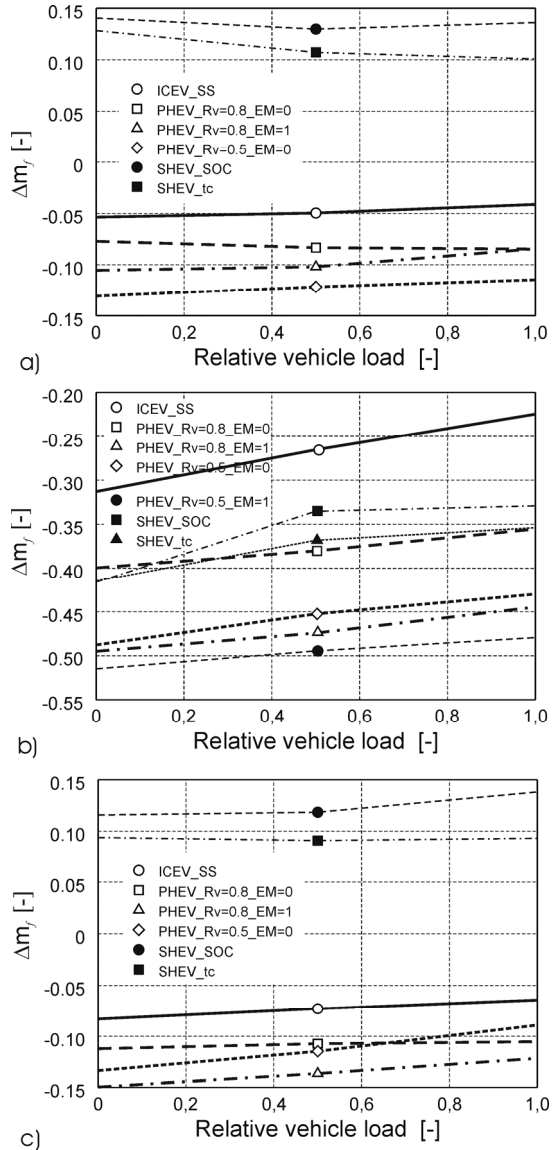
a)

b)

c)

Fig. 4. Δm_f for different vehicle loads: a) ECE_NEDC_LOW, b) BUSRTE, c) UDDSHDV cycle

It can be seen from Fig. 4b that fuel economy improvement (Δm_f) of ICEV_SS and HEVs over ICEV is much larger for the BUSRTE cycle. This is mainly the consequence of a lower average load of the BUSRTE cycle originating from low average velocity and long vehicle stop periods (Fig. 2). ICEV thus features very low $\eta_{ICE,eff}$, a large amount of the energy consumed during idling and a relatively large amount of the energy consumed by the brakes and thus

Katrašnik, T.

dissipated to heat. It can be seen that all curves feature a positive slope, which is mainly the consequence of very low $\eta_{ICE,eff}$ of the empty ICEV enabling significant fuel economy improvements at low vehicle loads. The stop/start strategy enables large fuel economy improvement through increased $\eta_{ICE,eff}$, whereas Δm_f decreases with an increasing vehicle load since a relative amount of the fuel consumed during idling decreases. Moreover, regenerative braking posses significant potential for improving fuel economy due to frequent decelerations. Therefore, optimum fuel economy is shifted to the PHEV_Rv = 0.5_EM = 1 that features very high $\eta_{ICE,eff}$ and recuperates large amount of the energy by regenerative braking. EM_START strategy thus enables a significant increase in the energy conversion efficiency since energy consumed by the EM is mainly gained by regenerative braking.

By analyzing the results of the UDDSHDV cycle (Fig. 4c) it can be concluded that relative changes in fuel consumption are similar to those of the ECE_NEDC_LOW cycle, which is related to the similar average velocity. However, the average load of the UDDSHDV cycle is larger than the average load of the ECE_NEDC_LOW cycle due to more frequent and more severe accelerations (Fig. 2). Optimum fuel economy therefore moves to parallel HEVs incorporating ICEs with larger swept volume (larger R_V). This is mainly the consequence of more severe accelerations, which imply a higher energy flow through the EM for PHEV_Rv = 0.5_EM = 0 and thus increased losses due to charging the ES by the ICE. This case exposes that frequent operation at high powertrain loads favor powertrains applying ICEs with larger swept volume since losses due to charging the ES by the ICE become substantial if it is not possible to gain the majority of the electric energy by regenerative braking.

5 CONCLUSIONS

Fuel economy of different HEVs and ICEVs was analyzed by simulation and analytical analysis. A combined approach clearly interprets influences of different test cycles, HEV topologies, configurations, vehicle loads and control strategies on the energy consumption of the HEVs and on the energy flows on different energy paths. It, therefore, proves to be an

efficient tool for optimizing HEVs based on their target application. It has been shown that HEVs make a significant fuel economy improvement for the test cycles where ICEVs feature low effective efficiency of the ICE and for test cycles enabling significant recuperation of the energy by regenerative braking possible. It is discernable that drive cycle characteristics influence potential improvement in the fuel economy of HEVs over ICEVs more significantly than vehicle load. It has been shown that HEVs featuring the highest effective efficiency of the ICE and the largest amount of the energy recuperated by regenerative braking do not necessary feature the best fuel economy, since losses due to electric energy production, storage and consumption, and, in particular cases, losses due to increased vehicle mass significantly influence the fuel economy of HEVs. It is discernable from the results that test cycles featuring increased average power and decreased possibility of recuperating energy by regenerative braking clearly favor the parallel HEV topology over the series HEV topology. It has also been shown that increased average power of the test cycle shifts optimum fuel economy towards parallel hybrid powertrains applying ICEs with larger swept volume. It is discernable from the results that drive-away and vehicle propulsion by the EM at low powertrain loads is always desirable for parallel HEVs if electric energy consumed by the EM could be recuperated by regenerative braking and not by operating the ICE at higher output. Otherwise, a detailed analysis revealing influences of different mechanisms on the fuel economy is necessary to justify this operation mode.

6 NOMENCLATURE

F multiplication factor of the test cycle [-]
M torque [Nm]
m mass [kg]
n engine speed [rpm]
Q_{LHV} lower fuel heating value [J/kg]
$R_V=V_{downsized}/V_{baseline}$ swept volume ratio [-]
t time [s]
V swept volume of the internal combustion engine [m^3]
v velocity [m/s]
W energy [J]
η efficiency [-]

Subscripts:

b	baseline
BR	brakes, braking
eff	effective
EM	electric machine
ES	electric storage
F	fuel tank
f	fuel
G	electric machine operating in the generator mode
ICE	internal combustion engine
M	electric machine operating in the motor mode
max	maximum
P	power converter, parallel
PR	propulsion
S	series
TC	torque coupling
tc	test cycle
TR	transmission
W	wheel

Abbreviations:

FR	fuel rack position
HEV	hybrid electric vehicle
ICE	internal combustion engine
ICEV	vehicle driven by an internal combustion engine
ICEV_SS	vehicle driven by an internal combustion engine featuring start/stop functionality
OEOL	optimum engine operation line
PHEV	parallel hybrid electric vehicle
rhs	right hand side of the equation
SOC	state of charge
SHEV	series hybrid electric vehicle

7 REFERENCES

[1] Lukic, S.M., Emadi, A. (2004). Effect of drivetrain hybridization on fuel economy and dynamic performance of parallel hybrid electric vehicles. *IEEE transactions on vehicular technology*, vol. 53, no. 2, p. 385-389.

[2] Lee, H., Kim, H. (2005). Improvement in fuel economy for a parallel hybrid electric vehicle by continuously variable transmission ratio control. *Proc. Instn. Mech. Engrs., Part D, J. of Automotive Engineering*, vol. 219, p. 43-51.

[3] Katrašnik, T. (2009). Analytical framework for analyzing the energy conversion efficiency of different hybrid electric vehicle topologies. *Energy Convers. Manage.*, vol. 50, p. 1924-1938.

[4] Banjac, T., Trenc, F., Katrašnik, T. (2009). Energy conversion efficiency of hybrid electric heavy-duty vehicles operating according to diverse drive cycles. *Energy Convers. Manage.*, vol. 50, p. 2865-2878.

[5] Chan, C.C. (2007). The state of the art of electric, hybrid, and fuel cell vehicles, *Proceedings of the IEEE*, vol. 95, no. 4, p. 704-718.

[6] Chau, K.T., Wong, Y.S. (2002). Overview of power management in hybrid electric vehicles. *Energy convers. manage.*, vol. 43, p. 1953-1968.

[7] Katrašnik, T. (2007). Hybridization of powertrain and downsizing of IC engine - a way to reduce fuel consumption and pollutant emissions - Part 1. *Energy Convers. Manage.*, vol. 48, no. 5, p. 1411-1423.

[8] Katrašnik, T., Trenc, F., Rodman Oprešnik, S. (2007). Analysis of the energy conversion efficiency in parallel and series hybrid powertrains. *IEEE transactions on vehicular technology*, vol. 56, no. 6/2, p. 3649-3659.

[9] Pacejka, H.B. (2006). *Tire and vechicle dynamics*, 2nd ed. SAE International, Warrendale, PA.

[10] Wu, B., Lin, C.C., Filipi, Z., Peng, H., Assanis, D. (2004). Optimal power management for hydraulic hybrid delivery truck. *Vehicle System Dynamics*, vol. 42, no. 1-2, p. 23-40.

[11] National Renewable Energy Laboratory. ADVISOR Documentation.

Katrašnik, T.